Original scientific paper

Received: Jun 22, 2020
Accepted: Jul 10, 2020
DOI: 10.2478/rmzmag-2020-0010

Investigation of Metal-based Composites Vibration Properties Using Modal Analysis in Combination with Wavelet Transforms Under Imitation of Operational Loads

Preiskava vibracijskih lastnosti kompozitnega materiala s kovinsko osnovo z uporabo modalne analize v kombinaciji z valovno transformacijo pod imitacijo obratovalnih obremenitev

Dmitrii S. Molchanov[1,*], Heinz Palkowski[2], Sergey Chernyakin[1], Panagiotis G. Karagiannidis[3]

[1] Space Engineering Department, Samara National Research University, 34, Moskovskoye Shosse, Samara, 443086, Russia

[2] Faculty of Natural and Materials Science, Clausthal University of Technology, Agricolastraße 6, Clausthal-Zellerfeld, 38678, Germany

[3] Faculty of Technology, School of Engineering, University of Sunderland, Sunderland SR6 0DD, UK

* molchanovds63@gmail.com

Abstract

The present article is dedicated to the study of the vibration properties of metal-based composite materials and the application of the non-destructive testing method. The main modal parameters of the metal-based composites were investigated. For experimental determination of natural frequencies and modes of oscillations, the method of scanning laser Doppler vibrometry was used. For the numerical modal analysis, the finite element method was used. The material model was a layered composite with isotropic linearly elastic layers and metal layers. The task of identifying the material model was considered as the problem of minimising the discrepancy between the calculated natural frequencies and the experimental ones. The developed method can be recommended for the determination of parameters of material models for calculating the modal characteristics of polymer–metal sandwich sheets and metallic mono-materials composite products. Methodology for identifying models of elastic behaviour of polymer–metal composite materials, based on the results of the experimental modal analysis, is presented. Wavelet-based damage detection is also presented as an appropriate approach for the identification of integral conditions of the metal–polymer–metal composite

Povzetek

Predstavljen članek obravnava študijo vibracijskih lastnosti kompozitnega materiala s kovinsko osnovo in uporabo neporušitvene preiskovalne metode. V delu so bili obravnavani glavni modalni parametri kompozitnega material s kovinsko osnovo. Za eksperimentalno določitev naravnih frekvenc in načinov nihanja je bila uporabljena Dopplerjeva laserska vibrometrija. Metoda končnih elementov je bila uporabljena za numerično modalno analizo. Modelni material predstavlja plastni kompozit, ki sestoji iz izotropno linearno orientiranih elastičnih plasti in kovinskih plasti. Naloga določitve ustreznega modela sloni na rešitvi problema z minimizacijo neskladja med izračunanimi naravnimi frekvencami in eksperimentalno izmerjenimi frekvencami. Razvita metoda se lahko uporabi za določitev modelnih parametrov, predvsem za izračun modalnih lastnosti plastnih kompozitov iz polimernih in kovinskih plasti, kot tudi kovinskih mono-materialnih kompozitnih produktov. Metodologija identifikacije modelov elastičnega obnašanja polimerno-kovinskih kompozitnih materialov sloni na podlagi rezultatov eksperimentalne analize. Zaznavanje poškodb na osnovi vibracij je predstavljeno kot ustrezen pristop za prepoznavanje integralnih pogojev kompozitnih plastnih materialov

Open Access. © 2020 Molchanov D.S., Palkowski H., Chernyakin S., Karagiannidi P.G., published by Sciendo. BY-NC-ND This work is licensed under the Creative Commons Attribution-NonCommercial-NoDerivatives 4.0 License.

materials. Results of wavelet transform convolutions are presented.

Key words: vibration properties, laminated metal-reinforced composites, experimental modal analysis, wavelet transforms, laser vibrometry.

kovina-polimer-kovina. Predstavljeni so tudi rezultati konvolucijske valovne transformacije.

Ključne besede: vibracijske lastnosti, kompoziti ojačeni s plastjo kovine, eksperimentalna modalna analiza, valovna transformacija, laserska vibrometrija.

Introduction

Metal–polymer–metal (MPM) composites that consist of an aluminium or steel bases with oxides, nitrides or carbides reinforcements had several advantages over monolithic materials. Although in the past they were not so tough, more expensive and difficult to handle, current applications from MPMs become highly valuable. Possible applications made from these composites are interior parts, floor supports, fuselage parts, highly loaded surfaces as helicopter rotor blades, turbine fan blades, etc.

One of the current issues in using advanced composite materials in aircraft construction is to provide strength in different conditions of vibrations, typical for aviation materials. At considerable amplitudes of oscillations that can occur, for example, under resonance conditions, situations can lead to critical situations up to failure. To exclude resonance oscillations, it is necessary to calculate the modal characteristics in detail at the design stage: their natural frequencies and forms of oscillations. In the case when products made of new composite materials, this calculation is complicated by the lack of reliable data on mechanical characteristics. The main problem (in comparison with isotropic materials) is a large number of parameters to be included in the material model, as well as the fact that these parameters depend on the material layers, changing with the fibres direction, bond reinforcement and technological factors. For example, an orthotropic elastic material contains nine parameters. Their definition is a laborious task. Data on materials characteristics, given in the literature, are often contradictory, and in carrying out responsible calculations require additional verification. For the computational analysis of the stress–strain state and modal analysis structures, the finite element method (FEM) can be effectively used [1–3]. Another big issue is the control and diagnostics of such structures during operation. At present, all civil, mechanical and aerospace structures might be damaged by impacts, overloading conditions, fatigue and deterioration of material properties forced by environmental factors. Damages also place in question the ability of the structure to perform its basic functions. For these reasons, many structural systems undergo routine inspections and maintenance to ensure stable operation and extend the lifespan. Identification and further characterisation of material damages without ruining the integrity of the material are made by the means of non-destructive evaluation (NDE) or non-destructive testing (NDT) [4, 5]. For imitation of conditions that can occur during operation, cycle loading could be most appropriate. In detail, according to the test data if any stress concentrator is present, then the load that can cause failure after a certain number of cycles will be a decreasing function of these cycles. Delamination, cracks in matrix and fibres and many other irregularities can simultaneously exist in the structure. Irregularities can also influence each other and, as a result, lead to avalanche failures of the construction [6]. According to experimental data, due to uncertainties and assumptions that are inevitable in the complex application the correct FEM application requires verification and identification (adjustment) of finite element models. Under-identification of a finite element, the model should be taken a change in its parameters, which minimises the differences between the calculated and test data.

There are two main purposes of this work. The first one is the development of a methodology for identifying the parameters of the elastic behaviour, according to the results of the experimental modal analysis (EMA), by the example of the layered MPM composites. The second one is the assessment of data, acquired during the first part for evaluation of control and diagnostic method for MPM composites based on wavelet transforms.

Material and Methods

Metal-based (polyethylene/polypropylene) PP/PE core composites were used for this research. This type of MPM composites with PP/PE core is highly deformable under room temperatures. The production cost of such composites is the same as the production of the same mono-materials and approximately two times cheaper than the production of the aluminium mono-materials. High bending strength and the possibility to play with the

Table 1. *Reference samples (sandwich sheets and metallic mono-materials)*

Mono-materials				
Notation	Material	Thickness [mm]	Notation	Grade
St. 0.24	Steel	0.24	St. 0.24	TS245
St. 0.49		0.49	St. 0.49	TS245
St. 2		2.0	St. 2	NA
Sandwich				
	Thickness [mm]	Thickness [mm]	Skin	Core
RP	0.24/0.3/0.24	0.78	TS245	PP-PE
RH	0.49/0.3/0.49	1.28	TS245	
RF	0.49/0.6/0.49	1.58	TS245	
RD	0.49/2.0/0.49	2.80	TS245	
RW**	0.49/0.3/0.24	1.03	TS245	
RX***	0.49/0.3/0.24/0.3/0.24	1.57	TS245	

*Three-layered sandwich with skin sheets of 0.5 mm thickness and a 0.6 mm core layer.
**Three-layered sandwich with different thicknesses of the steel (same grade) skin sheet. The thickness of each side is given.

***Five-layered sandwich. The thickness of the outer steel sheets is given. This one should be compared with the three-layered RF due to the same metallic contribution and thicknesses but different distributions.

Table 2. *E-Moduli and Poisson's values of the mono-materials*

Mono-material	Thickness [mm]	E-Modulus [GPa]	Poisson's ratio
PP-PE	0.2/0.3/0.6	1.45	-0.45
TS 245	0.24	197	-0.247
TS 245	0.49	191	-0.276
TH 470	0.49	210	-0.264

type of energy absorption of the composite part show high potential for the implementation of such composites for industry needs (including driven and moving parts).

To enable investigating various parameters regarding the thickness ratio of the core and skin sheets of the sandwich materials as well as different mechanical properties, the following material combinations have been prepared for study. Objects of study are MPM sandwich and mono composites. Detailed information is presented in Tables 1 and 2. Similar samples are recommended by the ASTM standards for the determination of composite materials' mechanical characteristics during tension and fatigue testing [7, 8]. Samples with different thicknesses, mass and compound materials were tested. As an example, detailed results only for samples RX5L and RD1 are further presented.

Processing of the Sandwiches

The Sn-coated metal sheets used were of deep drawing quality (Tinplate® TS 245 – EU 1.0372) with thicknesses of 0.24 and 0.49 mm. The polymer was a PP/PE foil with thicknesses of 0.2, 0.3 and 0.6 mm. PP/PE represents 80% of the copolymer, and the rest 20% represents talc, rutile and barite. To produce different sandwich types, roll bonding process was used. First, the mono-materials were prepared by cleaning and

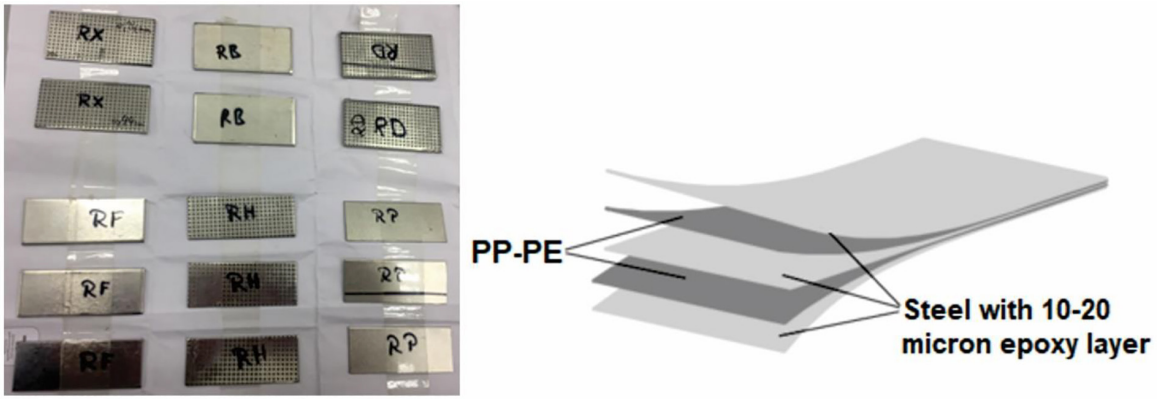


Figure 1. *Sample 'RX5L' (five-layered MPM sandwich composite; left top corner), before tests on the servo-hydraulic testing machine, and RX5L schematic structure of layers (right side figure).*

activating (polymer) and later bonded together in a two-step process using the epoxy resin Köratac FL201. The procedure is described in more detail in the study by Sokolova and others [9, 10]. For the five-layered sandwich, an additional step for preparing and activating the centre metal sheet was necessary, performing the same procedure used for the outer layers. The faultless production and quality of bonding were controlled by thermography and shear tests as described by Harhash et al. [11–13]. The Poisson's ratios of TS245 and TH470 were calculated by the width changes. Typical five-layered MPM sandwich composite among other samples is shown in Figure 1.

Theory/Calculation

The EMA is performed to obtain data about the natural frequencies and modes of oscillation, necessary for the subsequent identification of the computational model.

Modern EMA analysis, in particular, the method of scanning laser Doppler vibrometry, was used in this work. This method allows us not only to obtain high accuracy data on natural frequencies but also to determine forms of oscillations with high spatial resolution. The EMA method is based on the representation of the object under study as a vibrational system with a finite number of freedom degrees (n). The experimental determination of the natural frequencies of the system and the corresponding Eigenmodes is based on the analysis of the transfer function matrix [H], each element of which is the result of measurements of a separate frequency characteristic as the ratio:

$$H_{ij}(\omega) = \frac{X_i(\omega)}{Fj(\omega)},\ i,j = 1,\ \ldots,\ n \qquad (1)$$

where $X_i(\omega)$ is a frequency response function in the form of speed or acceleration for the i-th degree of freedom (DOF) it acts, when the $Fj(\omega)$ force corresponds to the j-th DOF and ω is the angular frequency. When using scanning laser vibrometry to one DOF of object i, an external force is applied and the response in the form of vibration velocity is measured in the set of DOF j = 1, …, n when they are sequentially scanned [14–16]. Later, according to Equation (1), the components of the transfer function matrix $H_{ij}(\omega)$ are determined. The natural frequencies are determined from the peaks on the measured amplitude–frequency response (AFR) of $H_{ij}(\omega)$. To determine their natural forms of oscillations one of the degrees of freedom is taken as the reference one, and a series of measurements of the vibration velocity amplitudes for all DOF is performed at the corresponding value of the modal frequency. The number of freedom degrees n for EMA is chosen for sufficient spatial resolution to provide a dependable presentation of the vibration modes.

The main advantage of the scanning laser vibrometry method is a non-contact measurement of vibrations, due to which the oscillation system is not exposed by additional factors

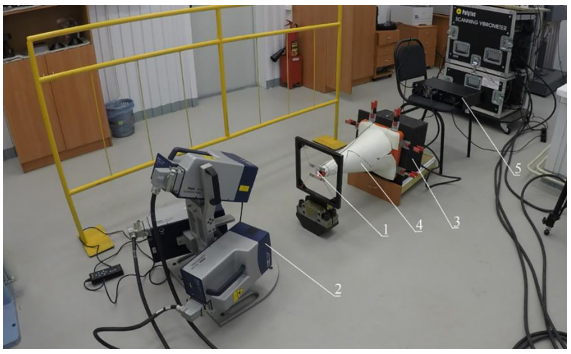


Figure 2. *Experimental facility: (1) sample, (2) three-headed laser Doppler vibrometer PSV-400, (3) acoustic oscillator, (4) acoustic diffuser and (5) amplifier.*

such as sensor masses or cable stiffnesses. It is not necessary to prepare or cut the sample or object for the test. Another advantage is the high spatial resolution: the density of the measurement points of the response is limited only by the accuracy of the laser focusing [13]. During EMA, a technique based on the Polytec PSV400-3D three-component scanning vibrometer [15–17] was used. It is a research laser-digital measuring complex, where the measurement of vibration velocity is based on the use of the Doppler effect. The PSV400-3D consists of three optical scanning laser heads, a geometry scanning module and a control system based on an industrial computer. The test sample was fixed on a rigid metal frame in compliant elastic suspensions (Figure 2).

Such scheme is often used in the EMA, which makes it possible to maximally approximate the fastening conditions to the absence of restrictions on movement ('free suspension'), convenient for reproduction in subsequent calculations. The oscillations were excited by means of specially designed acoustic dynamic. It generated a signal varying in time according to a harmonic law with a constant amplitude and a frequency (Periodic Chirp) and (White Noise) increasing to 6,000–6,400 Hz. Five experiments with different parameters of scanning net were executed for each sample. All of the tests were held in a quiet laboratory without any influential environmental noise sources. The performer started the timer to execute the experiment and left the laboratory in advance before each test. Due to the fact that vibration measured by the means of the laser Doppler vibrometer was caused by directed sound pressure in relatively small space, the influence of other minor measurement sounds in our case can be neglected.

For the calculation of modal analysis, the FEM was used. If we stated that the damping is neglected, the natural oscillations of the finite element model with (n) degrees of freedom can be described in matrix form (2).

$$[M]\left[\ddot{u}\right] + [K][u] = 0 \tag{2}$$

where $[M]$ is the mass matrix of the sample which depends primarily on its size, $[K]$ is the stiffness matrix of the sample, $[\ddot{u}]$ and $[u]$ are displacement and acceleration of the sample points, respectively. It should be noted that the stiffness matrix includes material parameters (elastic modules E and Poisson's ratios μ) and membrane and bending stiffnesses. In this case, since the sample is considered as a plate, we will have the expression for membrane stiffness in the form:

$$A = EF \tag{3}$$

where F is the cross-sectional area, and for the bending stiffness in the form:

$$D = \frac{Eh^3}{12(1-\mu^2)} \tag{4}$$

where h is the thickness of the sample.

Consequently, frequencies and waveforms will depend on both the material parameters and the sample configuration. The problem was solved by the FEM in the ANSYS Workbench software. It was assumed that the sample was free from restrictions on movement in a 'free suspension' state.

The task of identifying a material model is considered as an optimisation task with an objective function:

$$I = \sum_{i=1}^{n} a_i \left(\frac{f_{ip} - f_{ie}}{f_{ie}}\right)^2 \rightarrow min \tag{5}$$

where f_{ip} and f_{ie} are calculated and experimental values of (i) natural frequency and a_i are weight coefficients.

The control parameters are material characteristics, such as elasticity modulus and Poisson's

ratio. It is worth noting that during the manufacture of any material, researchers deal with the scatter of physical and mechanical characteristics. In particular, this means that these characteristics will change batch wise, i.e. they will be random variables. Therefore, it is impossible to guarantee that the material properties will ideally correspond to the passport data in Table 2. In addition, samples under study were made according to a certain technology. In particular, base carrier layers were rolled, and the parts of the construction were cured between each other by polymerisation process of thin epoxy layer. In this case, plastic deformation and heat treatment inevitably lead to a change in the properties of the final product.

According to the fact, that elasticity modulus, Poisson's ratio and layer thicknesses are included in the equation of vibration, i.e. they are the parameters on which the frequencies and modes of oscillations will depend. That is why, these parameters were chosen as the parameters to be optimised by Equation (5).

The weight coefficients in this equation were determined in accordance with the following approach: in the first step, for the selected *i*-th frequency, the a_i was adjusted in a way to satisfy Equation (5). The search for all frequencies here was performed independently from each other. After calculations at the first step of all a_i coefficients, their arithmetic average was found and then this coefficient was used as a weight coefficient to adjust the elastic modulus, Poisson's ratio and layer thicknesses depending on the exponent and the depending on which they enter Equation (5). At the second and at subsequent steps, the weight coefficients were selected based on a consideration of the mutual influence of frequencies on the value of Equation (5) in a way to satisfy the minimum condition of function I.

It is important that the calculated and experimental values of the natural frequencies correspond to the same own forms. In the present work, a comparison of the calculated and experimental natural (eigen) forms was carried out on the basis of an analysis of their animation representation.

For the construction of the finite element model, the finite elements of a volumetric body (SOLID185) with the option of a layered body were used. It should be noted that these elements provide modelling bulk bodies and can be used to simulate real structures. In addition, the use of the layered body option allows simulating layered bodies, in particular, composite materials. In this case, a multilayer material consists of several different materials. Special commands written in the programming language APDL (Ansys Program Design Language) set the material properties and the thickness for each layer. The finite element model of the object of study is presented in Figure 3. Table 3 presents the material characteristics and thicknesses of the layers in the sample multilayer structure which were obtained by the previously described method (Equation 5).

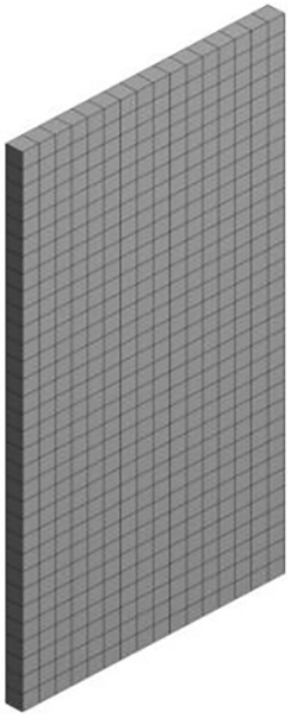


Figure 3. *Finite element model.*

Table 3. *Model parameters*

Mono-material	Thickness [mm]	E-Modulus [GPa]	Poisson's ratio
PP-PE	0.33	1.23	-0.39
TS 245	0.45/0.26	194/192	-0.245/0.3

Results and Discussion

Scattering of experimental data was estimated by the values of the coefficient of variation, which lies in the range of 0.59% (Table 4) and indicates the high accuracy of the experimental determination of the natural frequencies.
Sample vibration properties were measured (each 100,000 cycles) by means of three-headed scanning Doppler vibrometer until unstable conditions were detected. The vibration speed vector was calculated for a frequency range from 0 to 6,400 Hz. Graphs were compared.
Loading was executed by means of zero-to-tension stress cycle at the servo-hydraulic test machine SHIMADZU EHF-E (Figure 4), with the possibility of creating a wave of different shapes (sinus, triangle, straight, trapezium, 1/2 inversus, inclined plane, stepwise, arbitrary, sawtooth, oscillation, irregular) at frequencies from 10-5 to 102 Hz. In our case, we used the zero-to-tension stress cycle.
Cycle loading characteristics for sample RX5L (each iteration): frequency = 80 Hz; force = 1.265 kN; cycles count = 105.

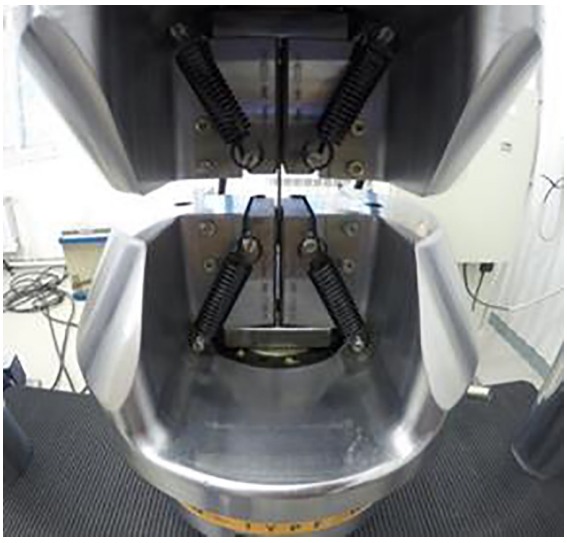


Figure 4. *Servo-hydraulic testing machine with a sample.*

Table 4. *Scattering of experimental data*

No.	Number of test/amount of scanning points					Average value	Coefficient of variation*
	1/25	2/51	3/51	4/165	5/165		
1	361	361	360	365	365	362.4	0.59
2	994	997	998	998	998	997	0.15
3	1,761	1,764	1,764	1,762	1,762	1,762.6	0.06
4	1,934	1,946	1,941	1,941	1,944	1,941.2	0.20
5	3,177	3,182	3,177	3,182	3,181	3,179.8	0.07
6	3,542	3,550	3,556	3,548	3,549	3,549	0.12
7	4,694	4,702	4,690	4,689	4,700	4,695	0.11
8	5,342	5,378	5,372	5,374	5,381	5,369.4	0.26

Note: Five experiments were carried out with various parameters of the scanning grid, which included from 25 to 165 points.
**A measure of the relative spread of a random variable, which shows that proportion of the average value is its average spread.*

To avoid irreversible changes in the material (sample) associated with plastic deformations, the loading level was selected on the lined area of the material (stress–strain) diagram (Figure 5). Analysing the corresponding diagrams, it was concluded to select the stress load at the level of 30 MPa for all samples.

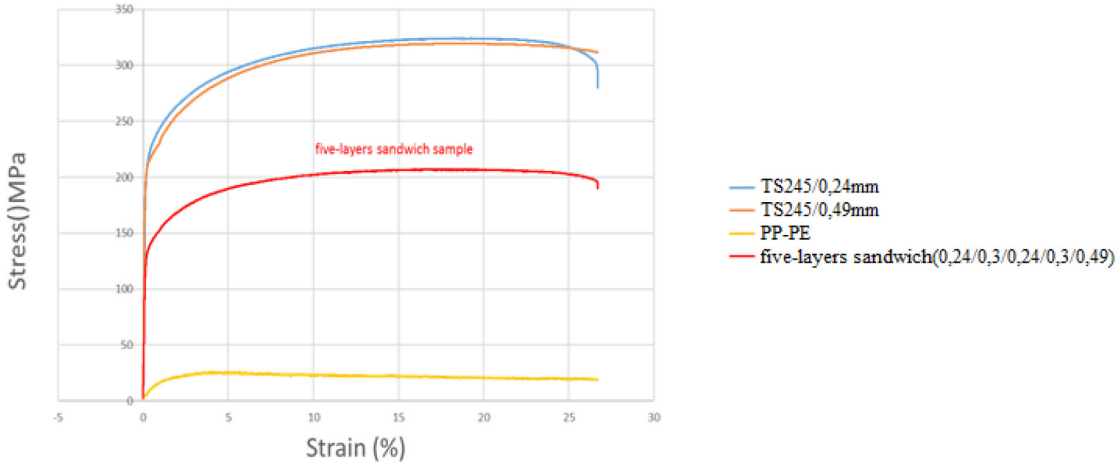


Figure 5. *Stress–strain diagrams for materials of tested samples.*

Table 5 presents the results of experimental testing (vibration vector, three heads) and computer modelling results for the five-layered sample 'RX5L'. Natural mode shapes test values and natural mode shapes FEM calculation are presented in Figures 6 and 7, respectively. The legend for FEM calculation is shown in Figure 8.

Table 5. *Test and FEM calculation values of natural modes shapes and frequencies for sample 'RX5L'*

No.	Test value		FEM calculation		Deviation [%]
	Natural mode shape (experiment)	Natural frequency [Hz]	Natural mode shape (FEM)	Natural frequency [Hz]	
1	Figure 6a	144	Figure 7a	128	12.5
2	Figure 6b	163	Figure 7b	177	7.90
3	Figure 6c	200	Figure 7c	189	5.82
4	Figure 6d	469	Figure 7d	416	12.74
5	Figure 6e	700	Figure 7e	798	12.28
6	Figure 6f	990.5	Figure 7f	1,113	11
7	Figure 6g	1,283	Figure 7g	1,441	10.96
8	Figure 6h	1,553	Figure 7h	1,480	4.93
9	Figure 6i	1,811	Figure 7i	1,732	4.56
10	Figure 6j	3,070	Figure 7j	3,503	12.36
11	Figure 6k	4,838	Figure 7k	4,365	10.83
FEM, finite element method.					

Mode shapes of RX5L sample were very similar in connection with translocation on frequencies. This gives us the right to judge that the experiment was quite clear. After second and third iterations at 300,000 cycles, the graphs show small differences. After fourth iteration at 400,000 cycles, there was an obvious translocation at high-frequency ranges.

Vibration properties of 'RD1' (three-layered sandwich) sample were measured (each 100,000 cycles) by means of three-headed scanning Doppler vibrometer until unstable

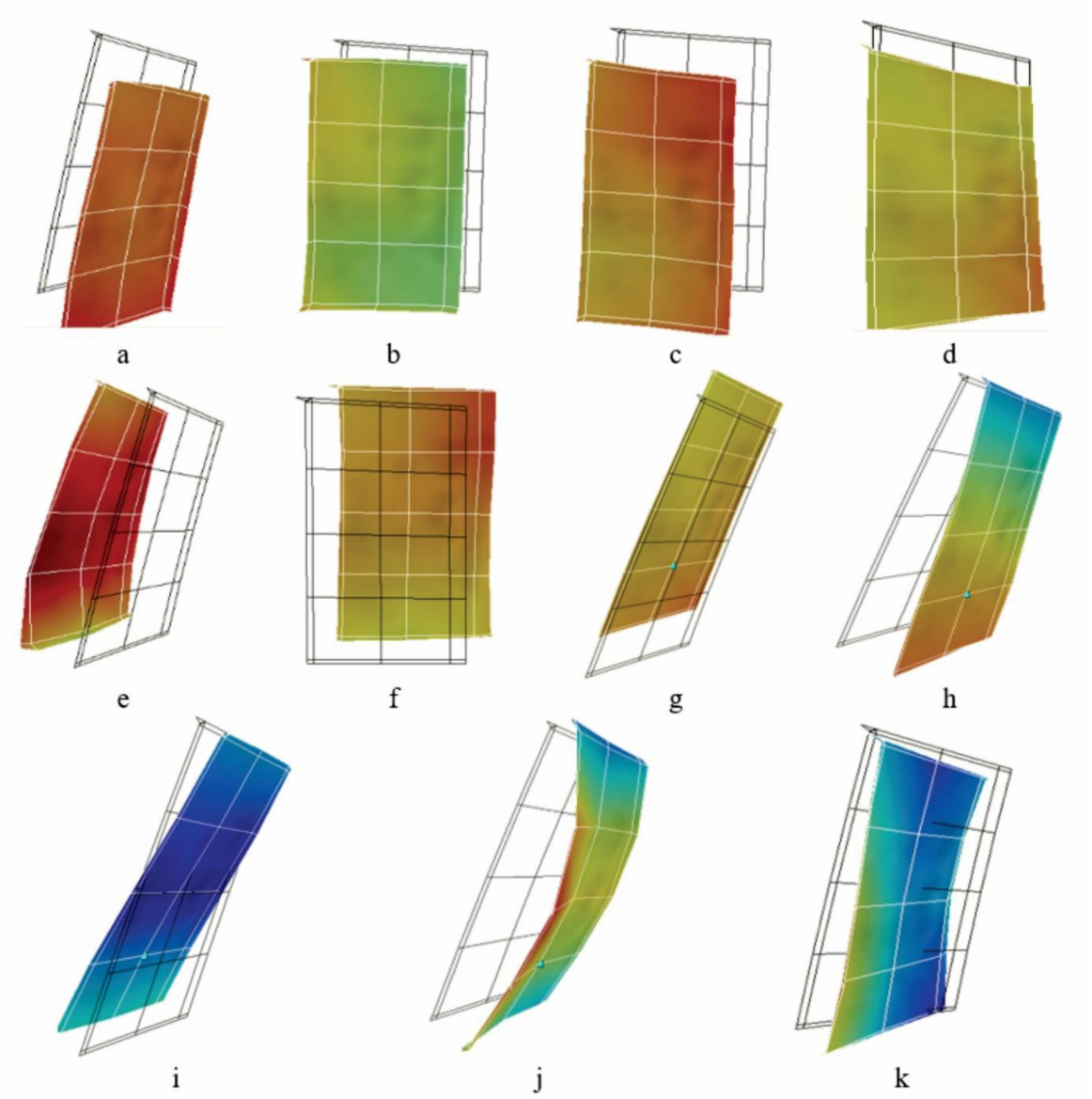


Figure 6. *Natural mode shapes: Doppler laser vibrometry experimental results.*

conditions were detected. The vibration speed vector was calculated for a frequency range from 0 to 8,000 Hz. Cycle loading characteristics (for each iteration) were: frequency = 80 Hz; force = 2.25 kN; cycles count = 100,000. Results were completely the same as with the five-layered sample, specifically the modal shapes were very familiar in connection with translocation on frequencies which also gave the confidence to judgement that the experiment was quite clear. As for RX5L sample after second and third iterations at 300,000 cycles, the graphs for the RD1 sample had small differences (in comparison with its original condition). Also after fourth iteration at 400,000 cycles, there was an obvious translocation at high-frequency ranges.

Further experiments have proved the fact that the change of vibration speed picture became enough predictable for the future forecast (Figure 9). It was found that the reference mode shapes at resonance frequencies are practically the same as with samples after 100,000–800,000 cycles loading. Another situation is with the amplitude at resonance frequencies for samples after loading of 100,000–400,000 cycles in comparison with the reference sample. Vibration speed vector

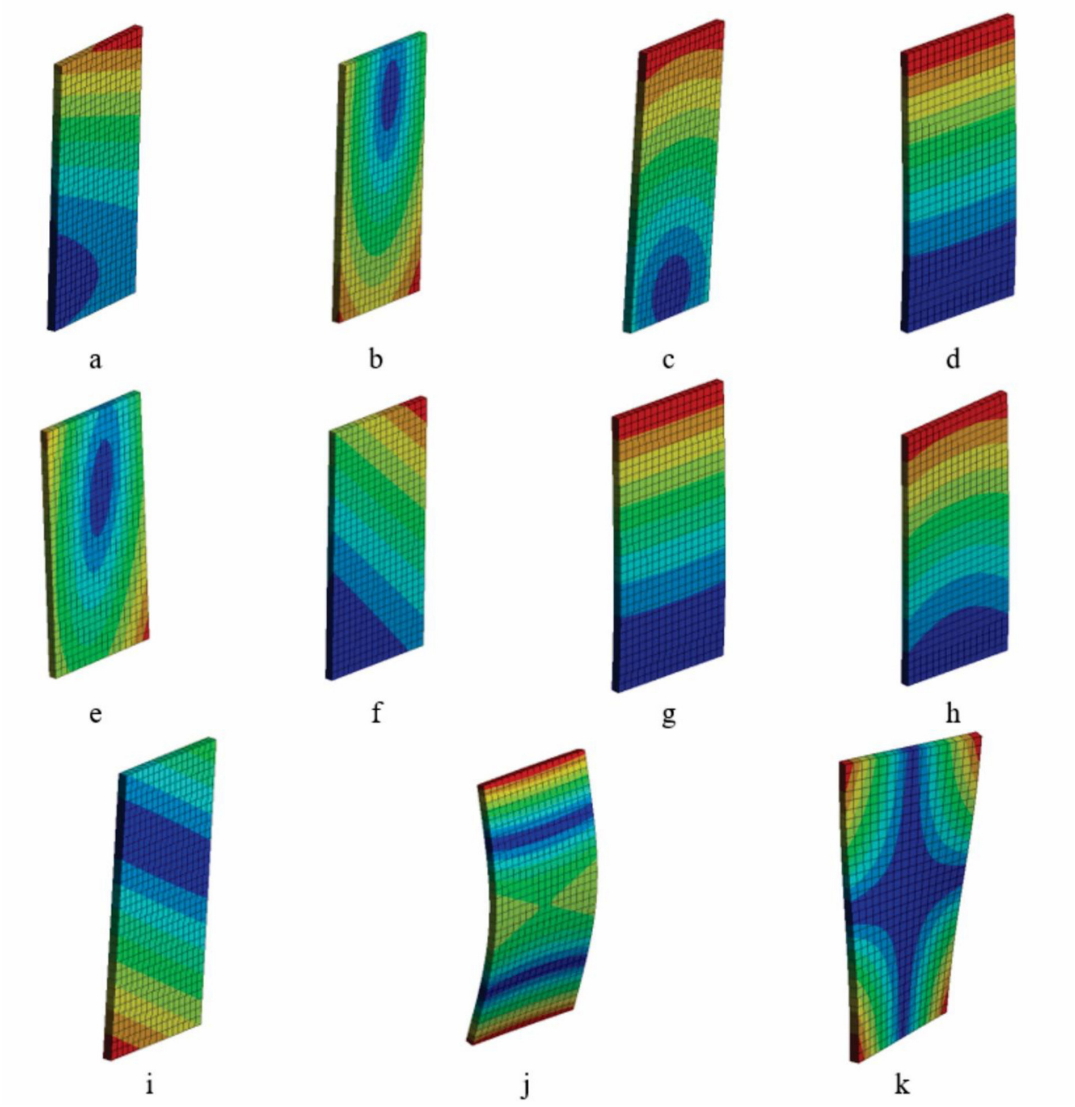


Figure 7. *Natural mode shapes: FEM calculation.*

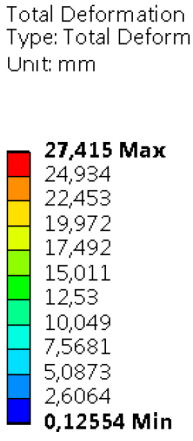


Figure 8. *Legend for finite element method calculation.*

diagrams, presented in Figure 9, shows the difference between the original and further conditions. There is an increase in the amplitude at low frequencies of approximately 30% and a sharp increase in the amplitude at frequencies above 500 Hz (equal to more than 100% of the amplitudes of the original samples at the same frequencies).

This research indicates that wavelet-based NDE analysis could provide a basis for determining damage levels in structural composite aerospace components, and thus being a means to decide whether a component is still operational. It is worth mentioning that the transformed signal reflects the overall picture of registered

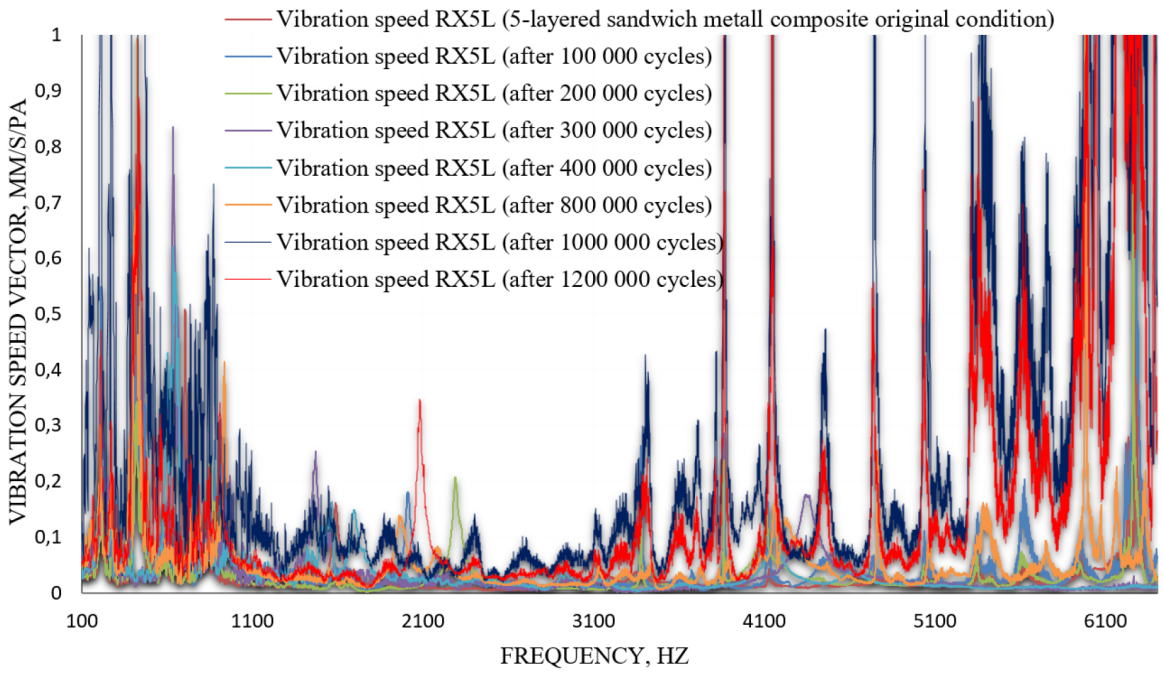


Figure 9. *'RX5L' (five-layered sandwich) vibration speed vector–frequency diagram.*

vibration. Briefly, wavelets are functions that can be applied to the signal function to search for different deviations. Opposite to Fourier transforms that can give information mostly at frequency domain, wavelet transforms allow getting information both at frequency and time domains. The transformed signal can be presented as three-dimensional (3D) plot of amplitude as a function of scale and translation. In our case, constant translation with variation only on scale parameter was accomplished. Additional basic theory information on wavelets can be found in the study by Molchanov and others [19, 20].

Based on the proposed algorithm, Fourier transformation is separately used for the determination of certain frequencies and resonance picture evaluation. Only the combination of these techniques can give affordable information for the interpretation of the obtained results. The same behaviour of vibration speed vector functions can be seen with all tested samples. It should also be mentioned that stress–strain diagrams were checked during each iteration (see Figures 10 and 11). It should be mentioned that by the value of the hysteresis loop space, we can also estimate the work spend on damage accumulation (the lower the space, the lower the work).

Experiments were executed until critical conditions. As an example, a five-layered sample was broken after 1,263,200 cycles. Stress–strain diagram at 63,200 cycles (seven load iteration for RX5L sample) is presented in Figure 12.

The second part of the article is devoted to the simplified method of obtaining amplitude response in combination with using Fourier and wavelet transforms. Additional detailed and basic information on the used method of wavelet transforms and data on vibration diagnostic signs acquired in previous works can be found in Molchanov and others [18, 19].

The presented experimental facility contains almost the same equipment (Figure 13). The main difference is the use of a one-headed laser Doppler vibrometer PDV-100, USB-4431 sound and vibration device and average processing capacity notebook. USB-4431 (102.4 kS/s, 100 dB, 0.8 Hz AC/DC coupled, 4-Input/1-Output Sound and Vibration Device) designed for sound and vibration measurements. Input channels incorporate integrated electronic piezoelectric (IEPE) signal conditioning for accelerometers and microphones. The four

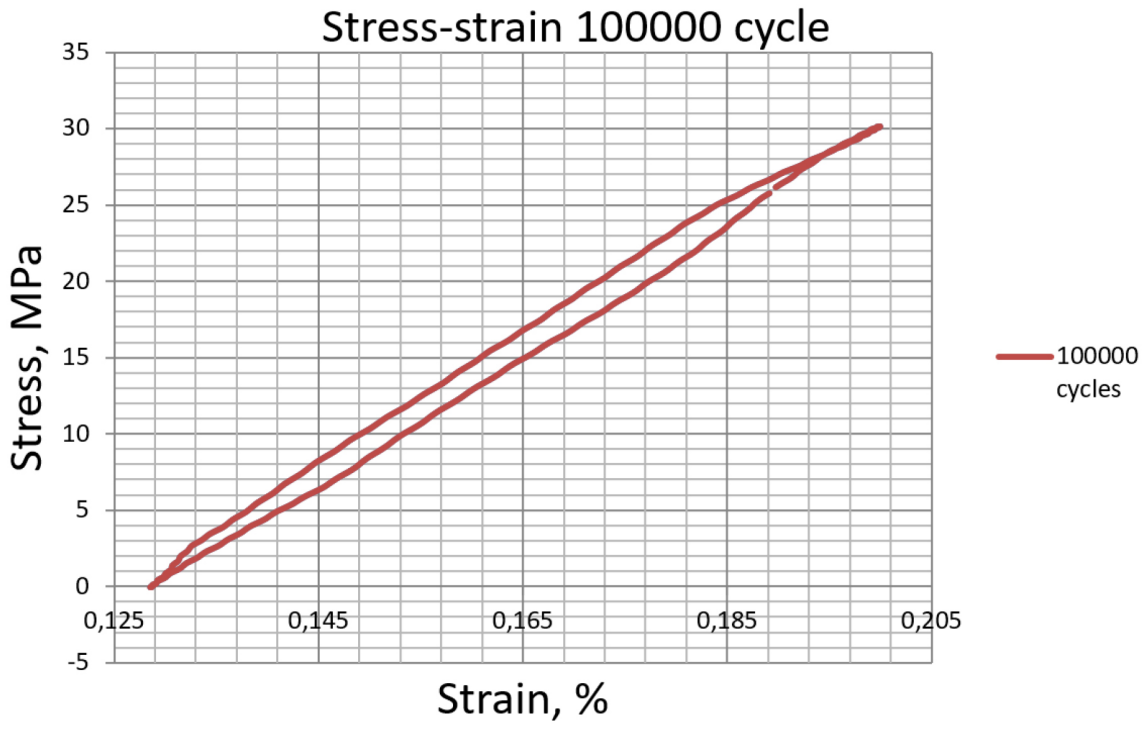


Figure 10. *Stress–strain 100,000 cycles for sample 'RX5L' (five-layered sandwich).*

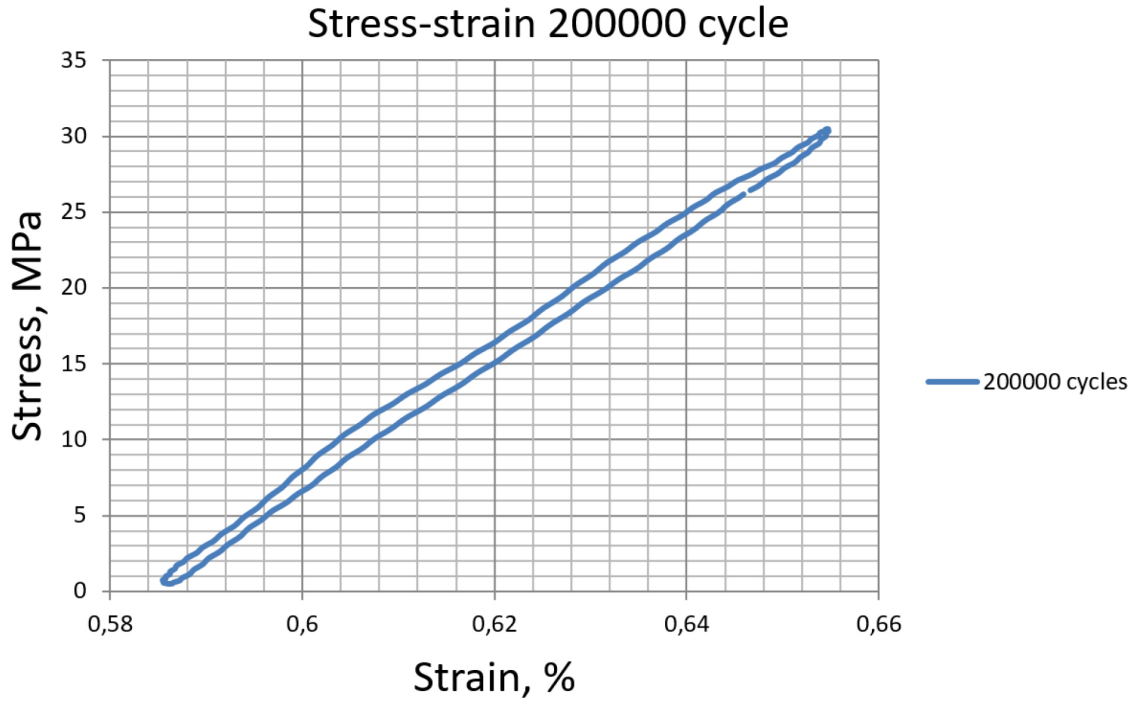


Figure 11. *Stress–strain 200,000 cycles for a sample 'RX5L' (five-layered sandwich).*

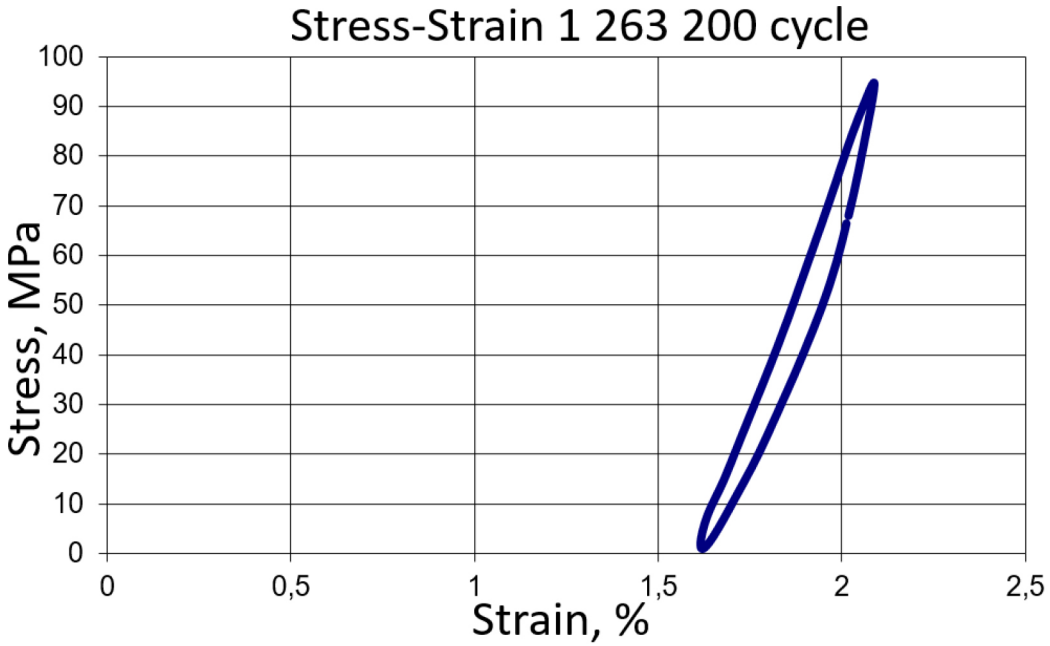


Figure 12. *Stress–strain diagram for a sample 'RX5L' (five-layered sandwich) during the break.*

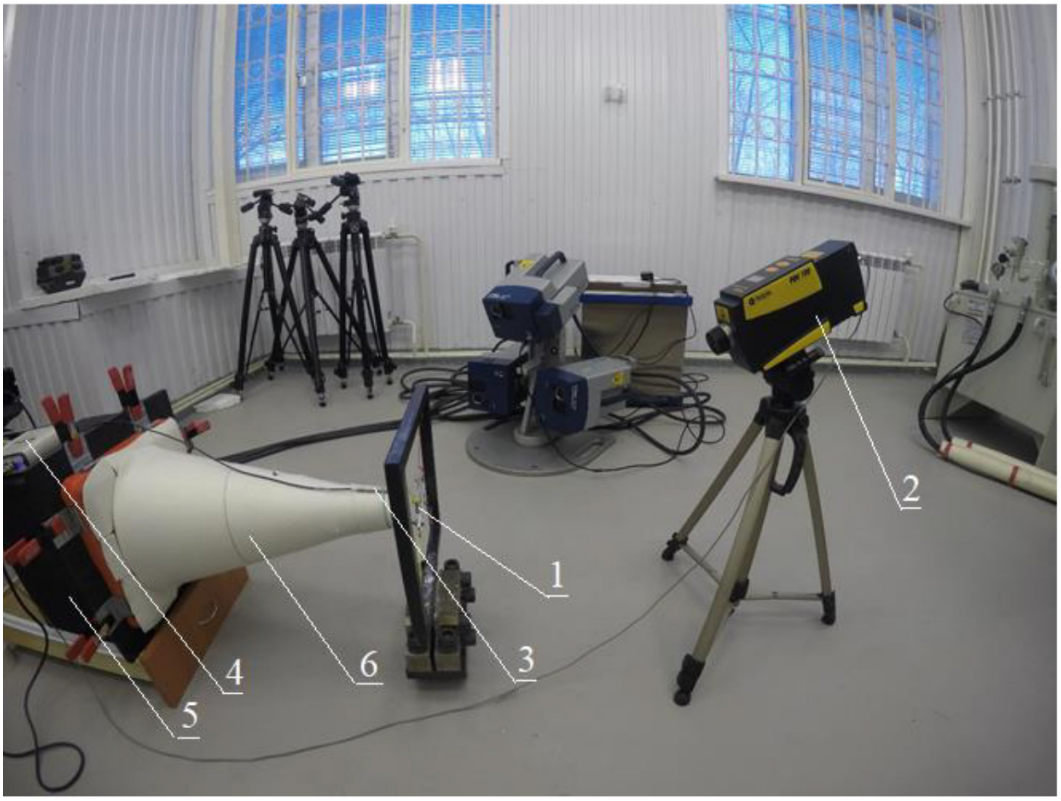


Figure 13. *Experimental facility: (1) sample, (2) one-headed laser Doppler vibrometer PDV-100, (3) microphone, (4) NI-USB-4431, (5) acoustic oscillator and (6) acoustic diffuser.*

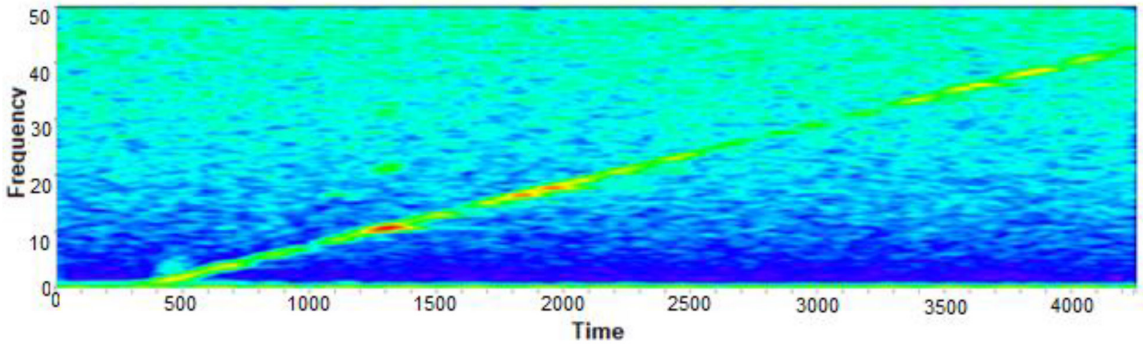


Figure 14. *Spectrogram of the reference sample RD1.*

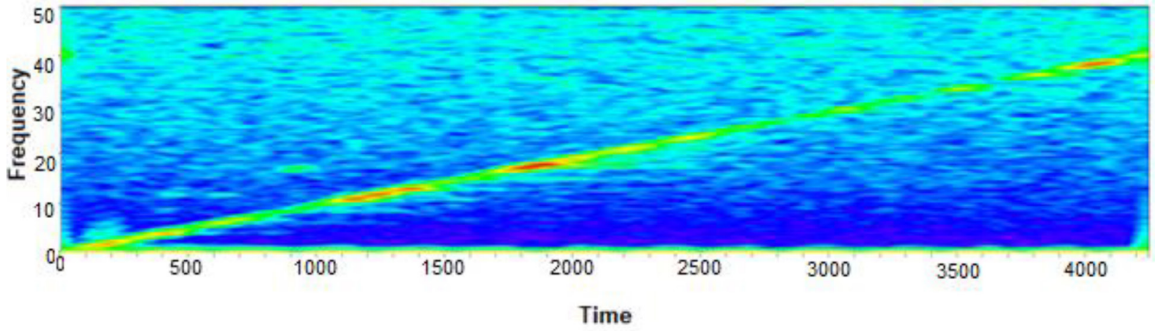


Figure 15. *Spectrogram of the sample RD1 after 100,000 cycles.*

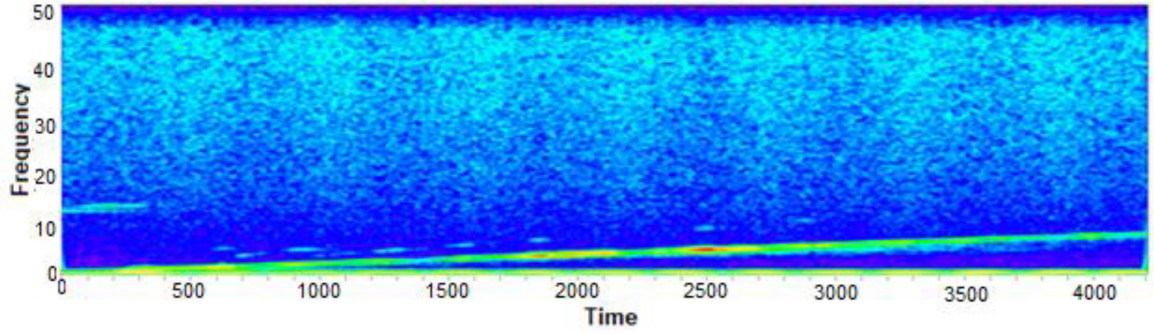


Figure 16. *Spectrogram of the sample RD1 after 300,000 cycles.*

USB-4431 input channels simultaneously digitise input signals. The analogue output (AO) channel is ideal for stimulus-response tests and it can be synchronised to the AI channels. After the measurement, recorded signals were put into written LabVIEW (Laboratory Virtual Instrumentation Engineering Workbench) program for calculation of Fourier spectrograms and wavelet transform convolutions. Another difference is the use of periodic chirp as generated sound in opposite to the white noise sound used in the first experimental part.

Results for the RD1 sample as spectrograms and 3D scalogram reflection after periodic chirp excitation (using one laser head) are presented in Figures 14–16. Signs of deterioration of the structure are natural frequency decline, damping of high frequencies, amplitude increase on a small scale, an increase in intensity at low frequencies, relevant frequencies 'Drift', the shift

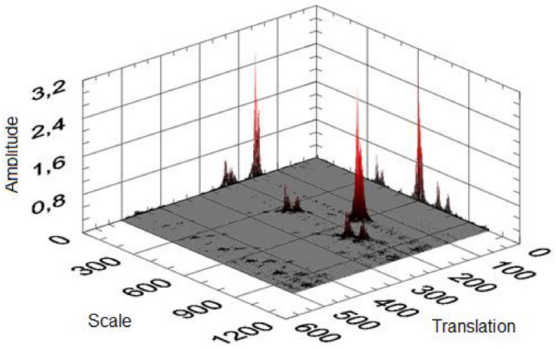


Figure 17. *Signals of sample RD1 after wavelet convolution (mother wavelet db02; scale 1024).*

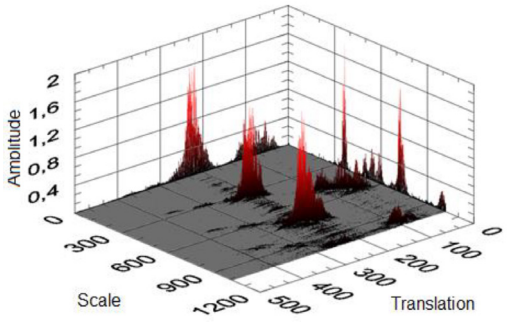


Figure 19. *The signal after wavelet convolution (mother wavelet db02; scale 1024). Sample RD1 after 200,000 cycles.*

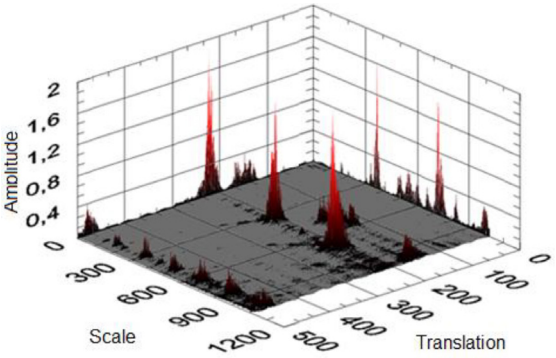


Figure 18. *The signal after wavelet convolution (mother wavelet db02; scale 1024). Sample RD1 after 100,000 cycles.*

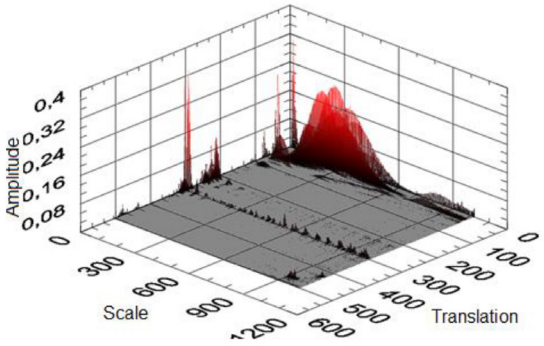


Figure 20. *The signal after wavelet convolution (used mother wavelet db02; scale 1024). Sample RD1 after 300,000 cycles.*

of the continuous wavelet transform (CWT) maximum towards larger scale (towards lower frequencies), low amplitude and absence of high frequencies (high frequencies could not be generated).

From the spectrum, it can be seen that a conventional sample spectrogram has higher values of vibration velocity than spectrograms after 100,000 and 300,000 cycles. Despite lower amplitude rise in time in comparison with the previous state, the increasing subharmonic activity with cycle load after each iteration can be seen. That is a direct sign that during use a more rapid failure under high vibration conditions is possible.

Visual features of 3D scalograms indicate changes in the overall vibration picture of the signal, which can describe the integral damage condition of the object itself. The wavelet transformed the function of the reference sample and it is presented in Figure 17. Further results are presented in Figures 18–20, respectively.

Signs of deterioration of the structure are natural frequency decline, damping of high frequencies, amplitude increase on a small scale, an increase in intensity at low frequencies, relevant frequencies 'Drift', a shift of the CWT maximum, overall low amplitude, absence of high frequencies (high frequencies could not be generated). With the increase of cycle loading after each iteration, the CWT picture changes strongly. This allows us to make a conclusion about typical signs occurring from 3D scalograms.

It is obvious that for each object the picture will be different, but there are changes that can be marked during the life cycle (as an example) to set the points in operation for maintenance checks. If the data can be collected statistically by means of many iterations (vibration tests) during operation and such deviations in connection with other parameters like resonance frequencies, this could give a reliable data on condition picture of the researchable object. Studies by Swiderski and his colleague [21, 22]

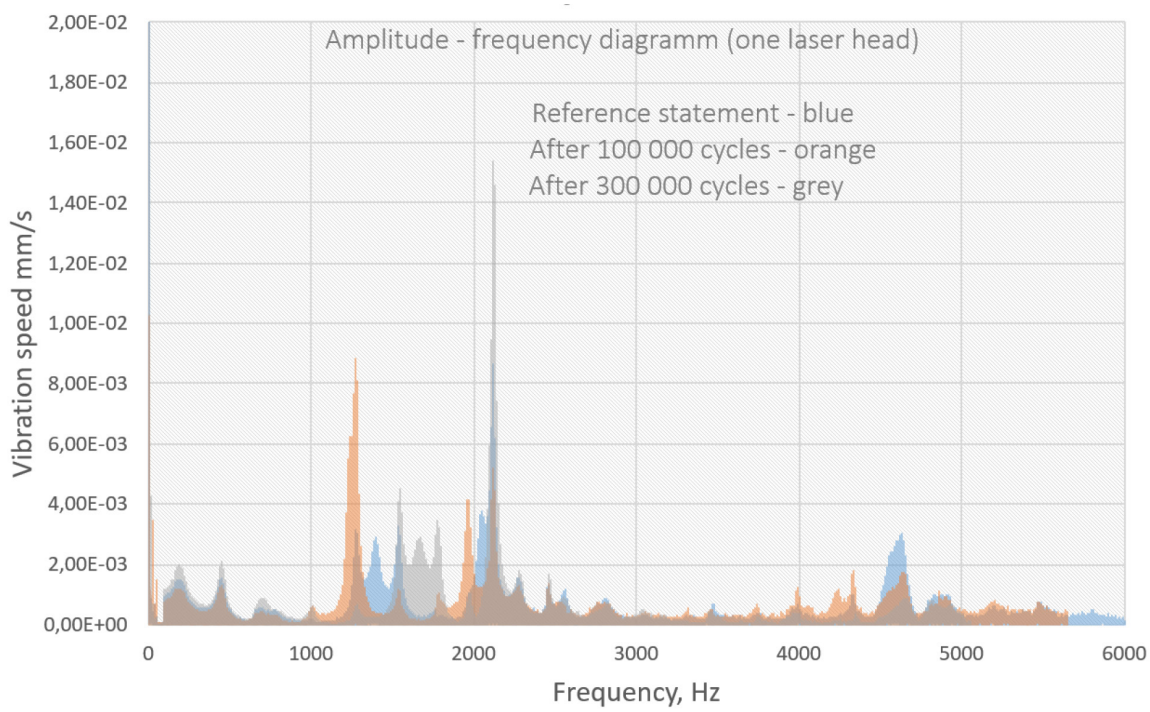


Figure 21. *Amplitude–frequency diagram. RD1 sample reference statement and after 100,000 and 300,000 cycles (one-headed Doppler laser vibrometer).*

contain additional information about experimental investigations of defect sizing in composite materials and different inverse and direct measurement problems.

The amplitude–frequency diagram (Figure 21) contains a comparison of data in the original condition and after 100,000 and 300,000 cycles for RD1. This diagram that was acquired at more simple equipment (by the means of one laser) also shows the tendency, when amplitude on certain frequencies changes according to forecast. It should be mentioned that vibration speed at frequencies close to 20–80 Hz was up to 0.06 mm/s (after 300,000 cycles), and the fact that amplitude growth at this low-frequency range was connected with cyclic loading.

Conclusion

During the calculation of modal characteristics (natural frequencies and vibration modes) of products made of polymer composite materials, it is necessary to exclude their resonance oscillations that requires reliable data on the mechanical characteristics of the material. The problem is a large (in comparison with isotropic materials) quantity of elasticity characteristics, and also in the fact that these parameters depend on a wide range of structural and technological factors.

One of this work purposes was to develop a methodology for identifying models of elastic behaviour of polymer–metal composite materials based on the results of the EMA. The object of investigation was layered reinforced sandwich sheets and metallic mono-materials.

The method of scanning laser vibrometry is used for experimental determination of natural frequencies and modes of oscillations. For the numerical modal analysis, the FEM is used. The material model is a layered composite with isotropic linearly elastic layers and metal layers. The task of identifying the material model is considered as the problem of minimising the discrepancy between the calculated natural frequencies and the experimental ones. To solve it, the quasi-random search method is used. The developed method can be recommended for the determination of parameters of material models for calculating the modal characteris-

tics of polymer–metal sandwich sheets and metallic mono-materials composite products.

For the EMA, a three-scanning and optimised one-scanning laser vibrometer were used; with its help, this work succeeded in obtaining semi-natural oscillation frequencies of samples, made from the metal composites in a frequency range up to 6,000 Hz with very insignificant scattering (overall average within 0.59%), and own forms with high space resolution.

Observation of the behaviour of five-layered samples under increasing of the load parameters led to the following conclusions. (1) The percentage ratio of certain material dictates its behaviour. Otherwise speaking, more percentage of the metal inside the construction shows more metal behaviour of the MPM composite as homogeneous substance. The opposite is true as well – more polymer shows more inhomogeneous behaviour. (2) Based on the experience with composite blades, it can be declared that for this type of MPM composites, significant amplitude increase at average frequency spectrum in combination with high damping of all other frequencies in the range from approximately 1,180 up to 3,050 Hz can be used as a diagnostic sign of unstable operation condition of the structure.

Similar to previous works with different elements made of composite material, obvious signs of alteration in CWTs were detected. The same features such as virtually unchangeable mode shapes at resonant frequencies after long cycle loading, natural frequency declines, damping of frequencies, amplitude increase on a small scale, an increase in intensity at low frequencies, shift of the CWT maximum, overall low amplitude were detected. According to tests and modelling procedures provided, metal-based composites are not an exception in behaviour. This research also indicates that wavelet-based NDE analysis in combination with complex modal analysis could provide a basis for determining damage levels in structural composite components, and thus a means to decide whether a component is still operational.

Acknowledgements

We gratefully thank for the financial support of the investigation within the project PA 873/42-1, financed by the DFG (German Research Community) and support of the Ministry of Education and Science of the Russian Federation. Moreover, we thank ThyssenKruppNirosta GmbH for delivering the metal sheets.

References

[1] Leontev, N.V. (2006): *Application of the ANSYS system to solving modal and harmonic analysis problems.* Nizhniy Novgorod Government University: Nizhniy Novgorod, 101 p.

[2] Laxalde, D., Thouverez, F., Sinou, J.J., Lombard, J.P., Baumhauer, S. (2007): Mistuning identification and model updating of an industrial blisk. *International Journal of Rotating Machinery*, vol. 2007, pp. 1–10, DOI: 10.1155/2007/17289.

[3] Grinev, M.A., Anoshkin, A.N., Pisarev, P.V., Shipunov, G.S., Nikhamkin, M.Sh, Balakirev, A.A., Konev, I.P., Golovkin, A.A. (2016): Calculation and experimental studies of the natural frequencies and vibration modes of the blade of a rectifying apparatus made from polymer composite materials. *PNRPU Mechanics Bulletin,* 4, pp. 106–119.

[4] Staszewkij, W., Boller, C., Tonlinson, G. (2004): *Health monitoring of aerospace structures*. John Wiley & Sons: West Sussex.

[5] Blanas, P., Das-Gupta, D.K. (2000): Composite piezoelectric materials for health monitoring of composite structures. In: *Materials Research Society Symposium - Proceedings*, Boston, Uchino, K., Ito, Y. (ed.). Cambridge University Press: Pennsylvania, pp. 45–50.

[6] Kassapoglou, C. (2012): *Predicting the structural performance of composite structures under cyclic loading*. Ph.D. Thesis. Harvard University, Faculty of Aerospace Engineering, Department of Aerospace Structures and Computational Mechanics: Cambridge, 140 p.

[7] Karabutov, A.A., Murashov, V.V., Podymova, N.B., Oraevsky, A.A. (1998): Nondestructive characterization of layered composite materials with a laser optoacoustic sensor. In: *Proceedings of Society of Photo-Optical Instrumentation Engineers*, Doctor, S.R., Nove, C.A., Daaklini, G.Y. (eds.). Society of Photo Optical, pp. 103–111.

[8] Kolodii, B.I., Lyaschuk, O.B. (1995): Direct and inverse problems of electromagnetic diagnostics of flat-laminated composite materials with the use of a rectangular waveguide. *Materials Science*, 30(2), pp. 173–181.

[9] Sokolova, O., Carradó, A., Palkowski, H. (2010): Production of customized high-strength hybrid sandwich structures. *Advanced Materials Research*, 137, pp. 81–128.

[10] Sokolova, O. (2012): *Study of metal/polymer/metal hybrid sandwich composites for the automotive industry.* Papierflieger, 160 p.

[11] Harhash, M., Carradò, A., Palkowski, H. (2016): Deep- and Stretch-Forming of Steel/Polymer/Steel Laminates. In: *2. International Conference. "Euro Hybrid Materials & Structures"*, Hausmann, J., Siebert, M. (eds.). p. 69–74.

[12] Harhash, M., Carradò, A., Palkowski, H. (2016). Forming Potential of Low-Density Laminates. In: *Proceedings of Euro Hybrid Materials and Structures*, Hausmann, J.M., Siebert, M. (eds.). DGM: Stade, pp. 53–60.

[13] Harhash, M., Palkowski, H., Carrado, A. (2017): *Forming behaviour of multilayer metal/polymer/metal systems.* Technische Universität Clausthal: Clausthal, 186 p.

[14] Heylen, W., Lamens, S., Sas, P. (2003): *Modal analyses. Theory and testing*. Katholieke Universiteit Leuven: Leuven, 325 p.

[15] Vibration measurements of the aerospace industry [online]. Polytec, renewed 1/01/2020 [cited 1/15/2020]. Available on: *http://www.polytec.com*.

[16] Inozemtsev, A.A., Nikhamkin, M.Sh., Voronov, L.V., Gladkiy, I.L., Golovkin, A. Yu., Bolotov, B.P. (2010): Experimental and calculated modal analysis of fan blades of hollow structure. *Aviatsionnaya promyshlennost*, 3, pp. 8–11.

[17] Grinev, M.A., Anoshkin, A.N., Pisarev, P.V., Zuyko, V.Yu., Shipunov, G.S. (2015): Computer modeling of the mechanical behavior of a composite blade of an aircraft engine straightener. *PNRPU Mechanics Bulletin*, 3, pp. 38–51.

[18] Molchanov, D.S., Makaryants, G.M., Safin, A.I., (2017): Defect-caused alteration of a composite unit modal parameters. *Measurement: Journal of the International Measurement Confederatio,* 95, pp. 383–388, DOI: 10.1016/j.measurement.2016.10.011.

[19] Molchanov, D., Safin, A., Luhyna, N., (2016): Damage monitoring of aircraft structures made of composite materials using wavelet transforms. *IOP Conference Series: Materials Science and Engineering,* 153(1), pp. 1–9, DOI:10.1088/1757-899X/153/1/01.2016.

[20] Daubechies, I. (1992): *Ten lectures on wavelets*. Mathematics: Philadelphia, 341 p.

[21] Swiderski, W., Szudrowicz, M. (2014): Experimental investigations of defect sizing in composite materials by ir thermography methods. In: *Proceedings of the 16th European Conference On Composite Materials*, European Conference on Composite Materials, pp. 1–8.

[22] Swiderski, W. (2003): Lock-in thermography to rapid evaluation of destruction area in composite materials used in military applications. In: *Proceedings of SPIE - The International Society for Optical Engineering,* Tobin, Jr.K.W., Meriaudeau, F. (eds.). Society for Optical Engineering: Gatlinburg, pp. 506–517.